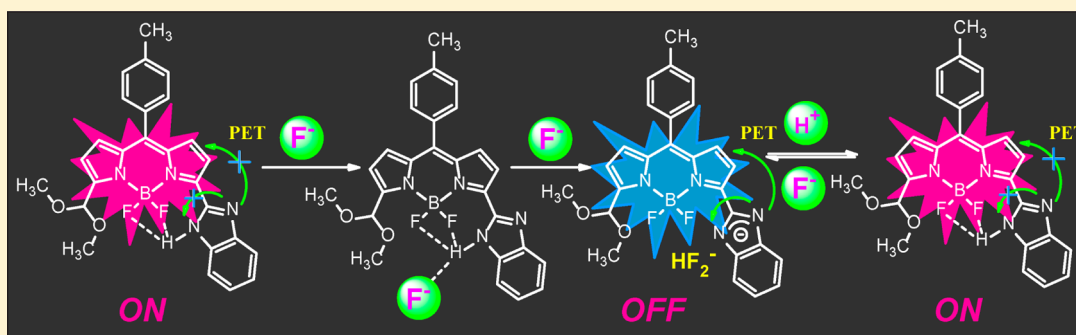


## Boron-Dipyrromethene Based Reversible and Reusable Selective Chemosensor for Fluoride Detection

Sheri Madhu and Mangalampalli Ravikanth\*

Department of Chemistry, Indian Institute of Technology Bombay, Powai, Mumbai 400 076, India

## Supporting Information



**ABSTRACT:** We synthesized benzimidazole substituted boron-dipyrromethene **1** (BODIPY **1**) by treating 3,5-diformyl BODIPY **2** with *o*-phenylenediamine under mild acid catalyzed conditions and characterized by using various spectroscopic techniques. The X-ray structure analysis revealed that the benzimidazole NH group is involved in intramolecular hydrogen bonding with fluoride atoms which resulted in a coplanar geometry between BODIPY and benzimidazole moiety. The presence of benzimidazole moiety at 3-position of BODIPY significantly altered the electronic properties, which is clearly evident in bathochromic shifts of absorption and fluorescence bands, improved quantum yields, increased lifetimes compared to BODIPY **2**. The anion binding studies indicated that BODIPY **1** showed remarkable selectivity and specificity toward F<sup>-</sup> ion over other anions. Addition of F<sup>-</sup> ion to BODIPY **1** resulted in quenching of fluorescence accompanied by a visual detectable color change from fluorescent pink to nonfluorescent blue. The recognition mechanism is attributed to a fluoride-triggered disruption of the hydrogen bonding between BODIPY and benzimidazole moieties leading to (i) noncoplanar geometry between BODIPY and benzimidazole units and (ii) operation of photoinduced electron transfer (PET) from benzimidazole moiety to BODIPY unit causing quenching of fluorescence. Interestingly, when we titrated the nonfluorescent blue **1**-F<sup>-</sup> solution with TFA resulted in a significant enhancement of fluorescence intensity (15-fold) because the PET quenching is prevented due to protonation of benzimidazole group. Furthermore, the reversibility and reusability of sensor **1** for the detection of F<sup>-</sup> ion was tested for six cycles indicating the sensor **1** is stable and can be used in reversible manner.

## INTRODUCTION

Fluoride is a common ingredient in anesthetics, hypnotics, psychiatric drugs, rat and cockroach poisons, and military nerve gases and is a contaminant in drinking water.<sup>1</sup> Excess fluoride exposure may cause collagen break down, bone disorder, thyroid activity, depression.<sup>2</sup> Thus, detection of fluoride with use of simple preparation and minimal instrumental assistance is desirable toward practical applications.<sup>3</sup> Various kinds of fluoride chemosensors have been developed based on urea<sup>4</sup> or thiourea,<sup>5</sup> amide,<sup>6</sup> phenol,<sup>7</sup> cationic borane,<sup>8</sup> pyrrole based macrocycles,<sup>9</sup> boron-dipyrromethenes (BODIPYs),<sup>10</sup> and so forth. Most of these sensors are normally irreversible and one time use for sensing fluoride ion.<sup>11</sup> A perusal of the literature reveals that there are very few scattered sensors available in the literature which can be used as reversible and reusable systems for sensing fluoride ion.<sup>12</sup> Our group is involved in the design and synthesis of new BODIPYs for sensing various anions and cations.<sup>13</sup> BODIPYs have very attractive features that include

sharp bands with large molar absorption coefficients in the absorption spectra, decent fluorescence quantum yields, reasonably long excited singlet state lifetimes, and good chemical and photochemical stability in both solution and solid states.<sup>14</sup> The properties of the BODIPY dyes can be fine-tuned by introducing suitable substituents at the right positions on the BODIPY core.<sup>15</sup> These dyes have numerous applications such as acting as light-harvesting arrays, biological probes, supramolecular fluorescent gels, fluorescent switches, and sensors.<sup>16</sup> In continuation of our work on BODIPYs, we have developed a new BODIPY based chemosensor **1** for fluoride ion which is found to be reversible and reusable as demonstrated by various spectroscopic techniques. Furthermore, BODIPY **1** also can be used as colorimetric sensor for F<sup>-</sup> ion, as it shows striking color change from fluorescent pink to

Received: November 5, 2013

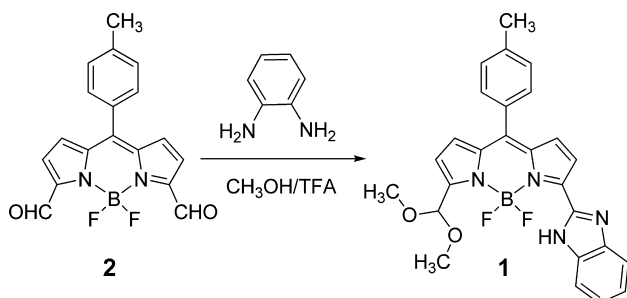
Published: January 22, 2014

nonfluorescent blue upon binding with  $F^-$  ion. Although several  $F^-$  ion sensors are available in the literature, the sensor reported here absorbs and emits in higher wavelength region and it is reversible compared to the earlier reported probes.

## RESULTS AND DISCUSSION

To synthesize the target BODIPY **1** (Scheme 1), we need access to 3,5-diformyl BODIPY **2** which was prepared by

### Scheme 1. Synthesis of BODIPY **1**



following our previously reported method.<sup>13a</sup> The reaction of **1** equiv of BODIPY **2** with **1** equiv of *o*-phenylenediamine in  $CH_3OH$  in the presence of a catalytic amount of trifluoroacetic acid at room temperature for 1 h. The progress of the reaction was monitored by TLC analysis, which showed complete disappearance of fluorescent yellow spot corresponding to BODIPY **2** with an appearance of a less polar, new pink fluorescent spot corresponding to the desired BODIPY **1** along with a minor spot corresponding to 3,5-bis(acetal) BODIPY. Column chromatography on basic alumina using petroleum ether/ethyl acetate (90:10, v/v) afforded BODIPY **1** as a golden yellow solid in 38% yield. The molecular ion peak at 473.1953 in high resolution mass spectra confirmed the identity of BODIPY **1** (Figure S1 in Supporting Information).  $^1H$  NMR;  $^1H$ – $^1H$  COSY; and  $^{13}C$ ,  $^{19}F$ , and  $^{11}B$  NMR spectroscopy were used to characterize compound **1** in detail (Figure S2–S7 in Supporting Information). Figure 1 shows the comparison of  $^1H$  NMR spectra of BODIPY **1** and **2** and  $^1H$ – $^1H$  COSY NMR spectrum of BODIPY **1**. In  $^1H$  NMR, BODIPY **2** showed two sets of signals for four pyrrole protons because of symmetric substitution. However, BODIPY **1** is unsymmetric and showed four sets of resonances for four pyrrole protons, which experienced upfield/downfield shifts compared to BODIPY **2**. All protons in  $^1H$  NMR spectrum of BODIPY **1** were identified based on the coupling constants, peak integration, and cross-peak correlations observed between the resonances in  $^1H$ – $^1H$  COSY (Figure 1) and NOESY spectra (Figure S7 in SI). In  $^1H$  NMR of BODIPY **1**, the  $-CH_3$  resonance appeared as singlet at 2.49 ppm showed cross-peak correlation with doublet resonance at 7.33 ppm in  $^1H$ – $^1H$  COSY spectrum which we identified as *c*-type *meso*-aryl protons. The *c*-type proton resonance at 7.33 ppm showed cross-peak correlation with multiplet resonance at 7.48 ppm in COSY spectrum which we recognized as *d*-type *meso*-aryl protons. The *d*-type protons in turn showed NOE correlation with doublet resonance at 7.59 ppm which corresponds to *a*-type pyrrole protons. The *a*-type protons showed cross-peak correlation with doublet at 7.05 ppm which we identified as *a'*-type pyrrole proton. Similarly, the *d*-type proton resonance at 7.48 ppm showed NOE correlation with doublet resonance at 6.96 ppm which we assigned to *b*-type pyrrole protons. The doublet resonance at

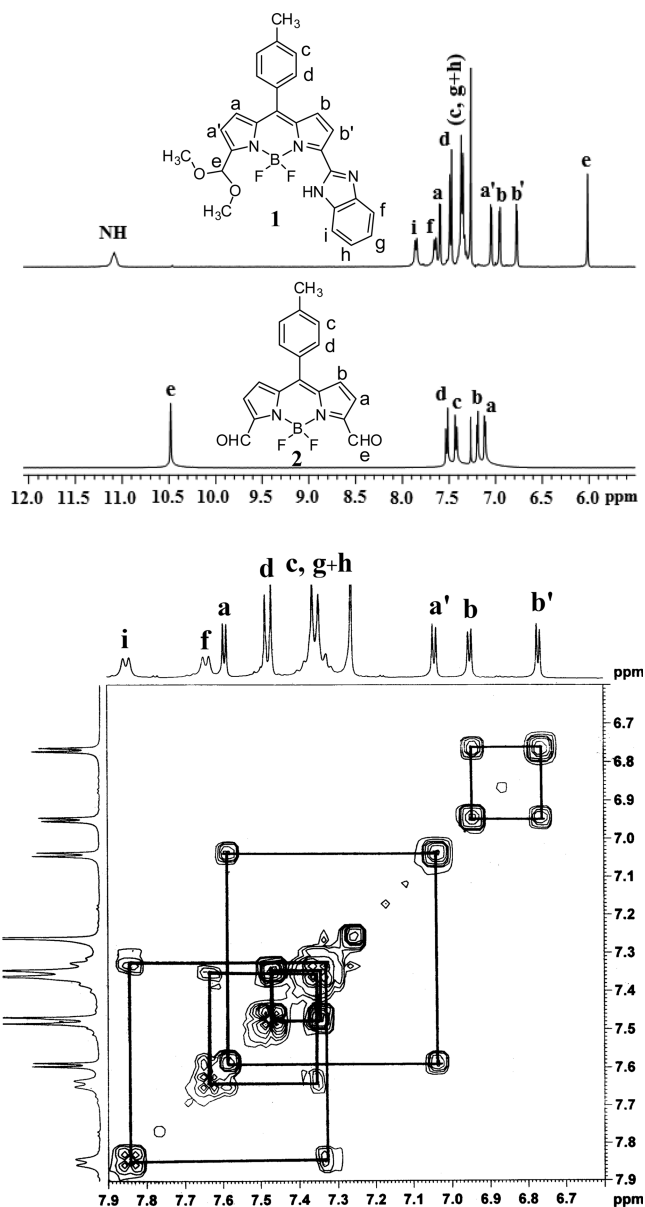


**Figure 1.** (a) Comparison of partial  $^1H$  NMR spectra of BODIPYs **1** and **2**. (b) Partial  $^1H$ – $^1H$  COSY NMR spectrum of BODIPY **1** recorded in  $CDCl_3$ .

6.76 ppm was assigned to *b'*-type pyrrole proton, as this resonance showed cross-peak correlation with *b*-type resonance at 6.96 ppm. The NH proton of benzimidazole moiety appeared as broad unresolved triplet at 11.08 ppm. The four aryl protons of benzimidazole moiety also identified similarly based on cross-peak correlations in 2D NMR spectra. The two doublets at 7.65 and 7.84 ppm corresponding to *f*-type and *i*-type protons, respectively, showed cross-peak correlation with multiplet resonance at 7.36 ppm, which corresponds to *g*-type and *h*-type protons. The  $-OCH_3$  protons of the acetal group appeared as a singlet at 3.51 ppm, whereas  $-CH$  proton appeared as a singlet at 6.01 ppm. Thus, 1D and 2D NMR spectroscopy were very helpful in deducing the molecular structure of BODIPY **1**. The BODIPY **1** showed a typical quartet at  $-137.7$  ppm in  $^{19}F$  NMR and a typical triplet at 0.31 ppm in  $^{11}B$  NMR spectra (Figure S4–S5 in SI).

We obtained single crystals for BODIPY **1** by slow evaporation of *n*-hexane/CHCl<sub>3</sub> (1:1 v/v) over a period of one week and crystallized in a monoclinic *P*2<sub>1</sub>/*c* unit cell. The crystal structure of BODIPY **1** (CCDC 969275) is shown in Figure 2. As shown in Figure 2, the BODIPY framework is

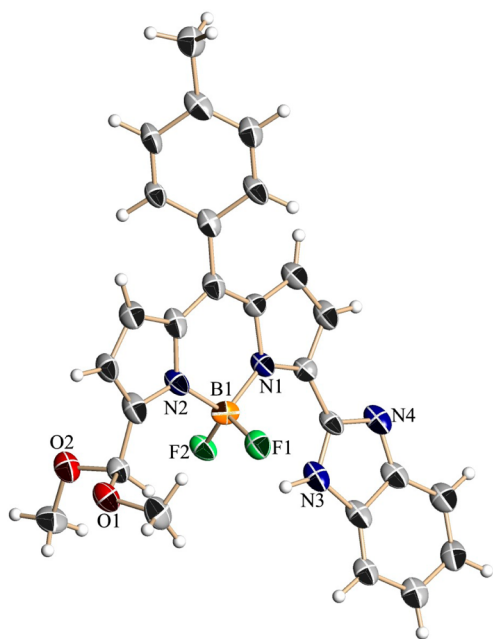


**Figure 2.** Molecular structure of BODIPY **1**. Thermal ellipsoids are drawn at the 50% probability level.

composed of two planar pyrrole rings and the central six-membered boron ring. The dihedral angle between the *meso*-aryl ring and the BODIPY core is 52° in BODIPY **1**. The B–N distances for BODIPY **1** are in the range of 1.54–1.55 Å, which indicates the usual delocalization of the positive charge. The benzimidazole moiety is also in the same plane as the BODIPY core. The striking feature of BODIPY **1** is the presence of intramolecular hydrogen bonding between the boron bound fluoride groups and the NH protons of the benzimidazole moiety. Each fluoride in BODIPY **1** is involved in hydrogen bonding with NH of the benzimidazole moiety with N–H...F distances are 2.45 Å (N–H3...F1) and 2.15 Å (N–H3...F2). The intramolecular hydrogen bonding helps the benzimidazole moiety and BODIPY core in one plane which led to effective electronic communication between the BODIPY core and the benzimidazole moiety.

#### Spectral and Electrochemical Properties of BODIPY **1**.

The absorption and emission properties of BODIPY **1** were studied in different solvents of varying polarity and relevant data is presented in Table 1. The absorption and emission

spectra of BODIPY **1** recorded in CHCl<sub>3</sub> are shown in Figure 3a. The absorption spectra of BODIPY **1** showed a characteristic strong band corresponding to a S<sub>0</sub>→S<sub>1</sub> transition at 580 nm with one vibronic component on the higher energy side at 540 nm which was clearly separated from the main transition. In addition, an ill-defined band at ~420 nm corresponding to a S<sub>0</sub>→S<sub>2</sub> transition is also present. The absorption study of BODIPY **1** in different solvents of varying polarity indicated that the absorption band is broad and weak and shifted to blue in polar solvents like CH<sub>3</sub>OH compared to nonpolar solvents like hexane in which the absorption band is relatively sharp and strong (Figure S8 in SI).

The BODIPY **1** showed strong emission band which is slightly Stoke-shifted and experienced a bathochromic shift of ~40 nm with decent quantum yield ( $\Phi = 0.31$ ) compared to BODIPY **2** ( $\Phi = 0.23$ ), indicative of a rigid structure of BODIPY **1** formed by an intramolecular hydrogen bonding between benzimidazole NH and boron-bound fluoride atoms (inset in Figure 3a). With the increase in the polarity of the solvent, the fluorescence band of BODIPY **1** was hypsochromically shifted and quantum yields were decreased. However, in the case of CH<sub>3</sub>CN and CH<sub>3</sub>OH, the BODIPY **1** showed strong fluorescence with a quantum yield in the range of 0.47–0.54. The singlet state lifetimes of BODIPY **1** in different solvents were measured using time correlated single photon counting (TCSPC) technique and the fluorescence decay of BODIPY **1** in different solvents were fitted to single exponential decay (Figure S9 in SI). The singlet state lifetime in different solvents is in the range of 1.8–6.2 ns. Thus, absorption and fluorescence studies indicated that the BODIPY **1** absorbs and emits in the visible region with very decent quantum yield and singlet state lifetime. The electrochemical properties of BODIPY **1** were followed by cyclic voltammetry in CH<sub>2</sub>Cl<sub>2</sub> using tetrabutylammonium perchlorate as the supporting electrolyte (Figure 3b). The BODIPY **1** showed one reversible and one irreversible reduction at –0.56 and –1.52 V, respectively, but did not show any oxidation. As clear from Figure 3b, the reduction waves of BODIPY **1** were shifted toward more negative by ~450 mV compared to BODIPY **2** indicating the BODIPY **1** is less electron deficient due to the presence of benzimidazole moiety.

**Sensing of Fluoride Ion.** It is well-known that the imidazole and benzimidazole contains hydrogen donor moiety like NH within the ring, which is useful for selective binding of anions, and BODIPY moiety is a good fluorophore. Therefore, the novel properties of benzimidazole and BODIPY in a single molecular framework was very useful to create a sensor in which the anion binding properties of benzimidazole can be monitored by following the changes in the spectral properties of BODIPY unit. We investigated the anion sensing ability of BODIPY **1** with various anions such as F<sup>–</sup>, Cl<sup>–</sup>, Br<sup>–</sup>, I<sup>–</sup>, OH<sup>–</sup>,

**Table 1.** Photophysical Data of BODIPY **1** Recorded in Different Solvents

solvent	$\lambda_{\text{abs}}$ (nm)	$\lambda_{\text{em}}$ (nm)	$\Delta\nu_{\text{st}}$ (cm <sup>–1</sup> )	log $\epsilon$	$\phi$	$\tau$ (ns)	$k_r$ (10 <sup>9</sup> s <sup>–1</sup> )	$k_{\text{nr}}$ (10 <sup>9</sup> s <sup>–1</sup> )	$\chi^2$
Hexane	581	592	320	3.32	0.38	5.2	0.073	0.119	0.98
CHCl <sub>3</sub>	579	596	493	3.93	0.31	4.7	0.087	0.147	1.00
CH <sub>3</sub> CN	568	591	685	3.59	0.47	5.8	0.081	0.091	1.04
C <sub>6</sub> H <sub>6</sub>	583	599	458	3.47	0.22	4.1	0.054	0.190	1.04
Toluene	583	599	458	3.33	0.20	4.3	0.047	0.186	0.99
MeOH	566	587	632	3.66	0.54	6.2	0.087	0.074	1.02
DMSO	575	601	752	3.56	0.18	1.8	0.100	0.456	1.08

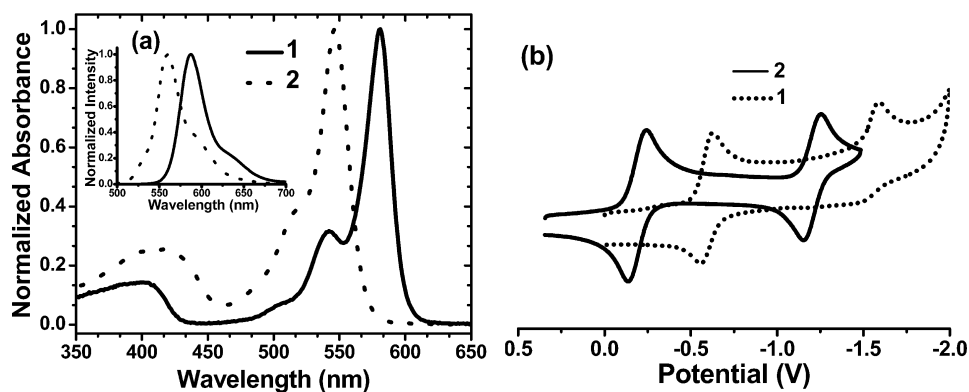


**Figure 3.** (a) Comparison of normalized absorption and emission spectra (inset) of BODIPYs 1 and 2 ( $5 \mu\text{M}$ ) recorded in  $\text{CHCl}_3$ . (b) Comparison of reduction waves of the cyclic voltammograms of BODIPYs 1 and 2 in dichloromethane containing 0.1 M tetrabutylammonium perchlorate as the supporting electrolyte recorded at a  $50 \text{ mV s}^{-1}$  scan rate.

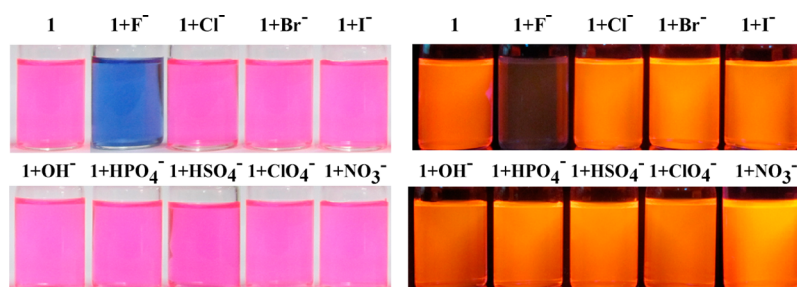


**Figure 4.** Color change induced upon addition of excess equivalents ( $7.5 \times 10^{-5} \text{ M}$ ) of various anions (tetrabutylammonium salts) to BODIPY 1 ( $5 \times 10^{-6} \text{ M}$ ) in  $\text{CH}_3\text{CN}$  solution under daylight (left) and UV lamp (right).

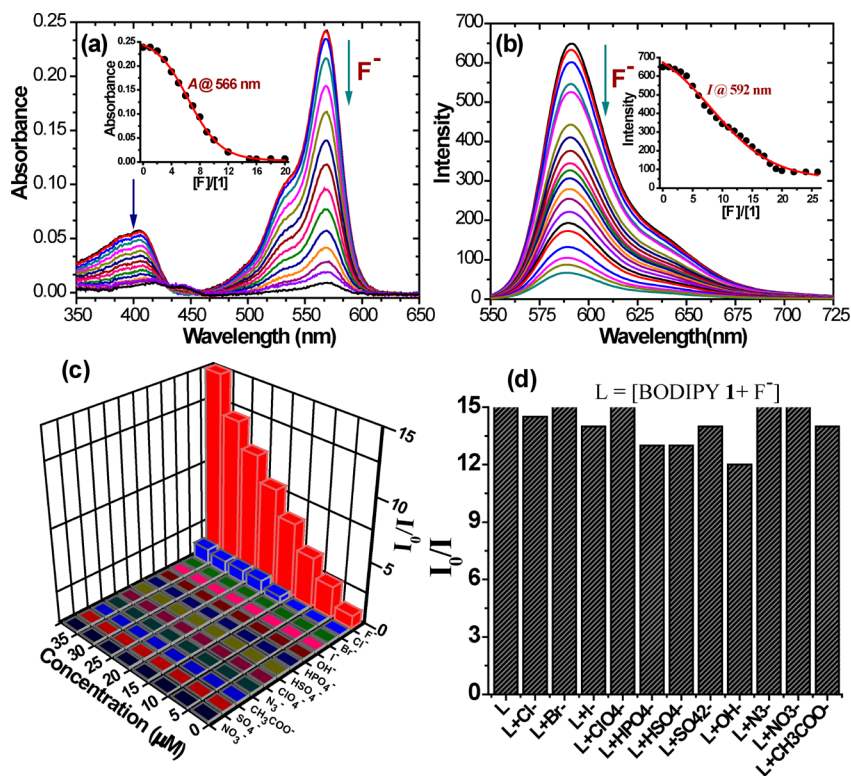
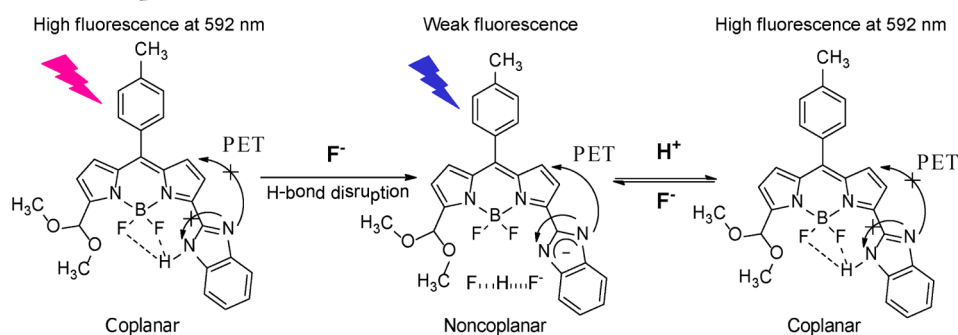


**Figure 5.** (a) Absorption, (b) emission spectral changes of BODIPY 1 ( $5 \mu\text{M}$ ) upon addition of increasing equivalents of  $\text{F}^-$  ions (0–15 equiv) in  $\text{CH}_3\text{CN}$  solution. The spectra were recorded after the addition of  $\text{F}^-$  ion to BODIPY 1 for 10 min. Excitation wavelength used was 530 nm. (c) Plots of relative emission intensity changes ( $I_0/I$ ) of BODIPY 1 ( $5 \mu\text{M}$ ) to  $\text{F}^-$  ion and common anions that could interfere with the emission intensity at different concentrations. (d) The histograms showing the competitive fluorescence titration response of BODIPY 1 in the presence of various other anions.  $\{[\text{BODIPY 1-F}^-] + \text{A}^{n-}\}$ ;  $[\text{BODIPY 1}] = 5 \mu\text{M}$ ,  $[\text{F}^-] = 15 \mu\text{M}$ ,  $[\text{A}^{n-}] = 30 \mu\text{M}$ .

**Scheme 2. Proposed Mechanism of Fluorescence On/Off for BODIPY 1 upon Addition of Fluoride Causes a Disruption of Intramolecular H-Bond and Operation of Photoinduced Electron Transfer Process**



$\text{HPO}_4^-$ ,  $\text{HSO}_4^-$ ,  $\text{SO}_4^{2-}$ ,  $\text{N}_3^-$ ,  $\text{ClO}_4^-$ ,  $\text{CH}_3\text{COO}^-$ , and  $\text{NO}_3^-$  (as tetrabutylammonium salts) in  $\text{CH}_3\text{CN}$  solution. Our visual inspection under both ambient and UV light showed that upon the addition of various above-mentioned anions (Figure 4), a discernible color change from fluorescent pink to non-fluorescent blue color of BODIPY 1 solution occurs only in the presence of  $\text{F}^-$  ion, which indicates that BODIPY 1 has the potential to act as specific sensor for  $\text{F}^-$  ion. We carried out the specific selectivity of BODIPY 1 for  $\text{F}^-$  ion by using various spectroscopic and electrochemical techniques.

**Selective Detection of  $\text{F}^-$  Ion by Absorption, Fluorescence, NMR and Electrochemical Studies.** The absorption spectral titration of BODIPY 1 was carried out by addition of increasing amounts of  $\text{F}^-$  ions in  $\text{CH}_3\text{CN}$  solution. The systematic changes in the absorption spectra of BODIPY 1 on addition of TBAF in  $\text{CH}_3\text{CN}$  are shown in Figure 5a. Addition of increasing amounts of  $\text{F}^-$  ion to acetonitrile solution of BODIPY 1 resulted in the significant decrease in the intensity of absorption bands at 568 and 420 nm with one clear isosbestic point at 428 nm supporting the binding of  $\text{F}^-$  ion to BODIPY 1. The changes in the absorbance at different equivalents of  $\text{F}^-$  ion were plotted and shown as an inset in Figure 5a. The sigmoidal nature of the plot serves as an indicator of analyte binding. Under identical conditions, the addition of various above-mentioned anions (excess equivalents) did not produce any changes in the absorption spectra of BODIPY 1 or color of the solution. Similarly, the selective sensing of  $\text{F}^-$  ion by BODIPY 1 was also followed systematically by fluorescence titration experiments. The BODIPY 1 is decently fluorescent with a quantum yield of  $\sim 0.5$ . Upon addition of increasing amounts of  $\text{F}^-$  ion, the fluorescence intensity of BODIPY 1 at 591 nm was gradually decreased and almost quenched in the presence of 15 equivalents of  $\text{F}^-$  ion in  $\text{CH}_3\text{CN}$  (Figure 5b). The significant changes in the fluorescent intensity of BODIPY 1 with a clear color change from fluorescent pink solution to nonfluorescent blue solution indicates the following: (i) the binding of  $\text{F}^-$  ion with benzimidazole NH atom resulted in the increase of electron density on imidazole moiety due to deprotonation, which causes the fluorescence quenching via photoinduced electron transfer (PET), and (ii) the binding of  $\text{F}^-$  ion leads to the disruption of hydrogen bond between fluoride atoms of BODIPY and benzimidazole moiety, which may result in noncoplanar geometry between BODIPY and benzimidazole causing quenching of fluorescence (Scheme 2). The association constant of BODIPY 1 by  $\text{F}^-$  ion was estimated by Stern–Volmer equation, and the corresponding association constant,  $K_a$ , was found to be  $3.1 \times 10^6 \text{ M}^{-1}$  (Figure S10 in SI). The

sensitivity of BODIPY 1 for  $\text{F}^-$  ion was further evaluated by using the linear dynamic response and the detection limit (LOD) was found to be 93 nM (Figure S11–S12 in SI).

To investigate the selective binding of  $\text{F}^-$  ion to BODIPY 1, fluorescence spectra of BODIPY 1 in the presence of various above-mentioned tetrabutylammonium anions were recorded. As shown in Figure 5c, only  $\text{F}^-$  ion induced a prominent intensity change, whereas addition of various other anions under identical conditions led to almost no change in fluorescence intensity, which clearly indicates that BODIPY 1 acts as a highly selective sensor for the detection of  $\text{F}^-$  ion over other anions. Moreover, competitive binding experiments performed by addition of excess amounts of other anions did not interfere with either the binding of  $\text{F}^-$  to the BODIPY 1 or the subsequent fluorescence quenching (Figure 5d), which demonstrates that BODIPY 1 can specifically detect  $\text{F}^-$  ions even in the presence of other analyte ions. We also tested the sensing behavior of BODIPY 1 with various other metal fluoride salts such as KF, CsF, and  $\text{HgF}_2$  (Figure S13 in SI). The studies showed that various metal fluorides showed similar spectral changes like TBAF indicating that counter cations do not play any role in the sensing of  $\text{F}^-$  ion. To determine the binding stoichiometry of BODIPY 1, fluorescence measurements were carried out in the presence of varying mole-fractions of  $\text{F}^-$  ion in acetonitrile (Figure S14 in SI). Job's plot analyses reveal a maximum at  $\sim 0.3$ , indicative of the formation of a 1:2 complex between BODIPY 1 and  $\text{F}^-$  ion.

The fluoride anion binding to BODIPY 1 was also monitored by  $^1\text{H}$  NMR titration studies in  $\text{DMSO}-d_6$ . The systematic changes in  $^1\text{H}$  NMR signals of BODIPY 1 upon addition of increasing amounts of fluoride ion were shown in Figure 6. As is clear from Figure 6 that upon addition of only 0.5 equiv of  $\text{F}^-$  ion, the signal corresponding to the benzimidazole NH proton experienced downfield shift and broadened. However, upon addition of 5 equiv of  $\text{F}^-$  ion, we noticed one triplet at  $\sim 16.7$  ppm suggesting the formation of  $\text{HF}_2^-$  ion which confirmed the deprotonation of the benzimidazole NH proton. The deprotonation of benzimidazole NH proton was also evident in the upfield shifts of various BODIPY core protons. Furthermore,  $^{19}\text{F}$  NMR titration spectra also provide clear evidence for interaction of  $\text{F}^-$  ion with BODIPY 1 upon titration with increasing equivalents of  $\text{F}^-$  ion in  $\text{DMSO}-d_6$  as shown in Figure 7. The sharp signal at  $-108$  ppm is due to the tetrabutylammonium fluoride titrant; i.e., the respective signal is due to unbound fluoride anions, whereas the BODIPY 1 showed a typical quartet at  $-137$  ppm. Upon addition of 1.5 equiv of  $\text{F}^-$  ion to BODIPY 1, the quartet signal intensity at  $-137$  ppm decreased and at the same time a new quartet signal

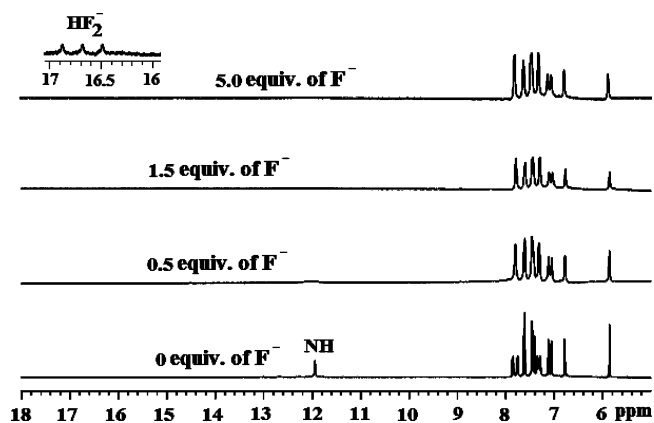


Figure 6. Partial  $^1\text{H}$  NMR titration spectra of BODIPY **1** ( $1.6 \times 10^{-2}$  M) upon addition of increasing amounts of  $\text{F}^-$  (TBAF) ion (0–5 equiv) in  $\text{DMSO-}d_6$ .

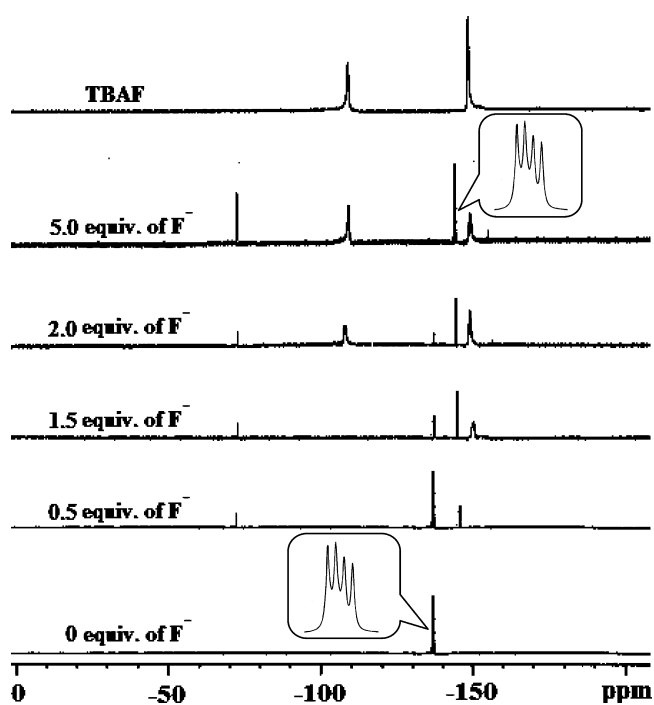


Figure 7.  $^{19}\text{F}$  NMR titration spectra of BODIPY **1** ( $1.6 \times 10^{-2}$  M) upon addition of increasing amounts of  $\text{F}^-$  (TBAF) ion (0–5 equiv) in  $\text{DMSO-}d_6$ .

at  $-145$  ppm appeared with equal intensity. However, upon addition of 5 equiv of  $\text{F}^-$  ion to BODIPY **1**, the signal at  $-137$  ppm completely disappeared and signal at  $-145$  ppm became prominent along with the formation of  $\text{HF}_2^-$  ion, which showed a clear signal at  $-148$  ppm.<sup>17</sup> This significant upfield shift of  $\sim 8$  ppm in  $^{19}\text{F}$  NMR spectrum clearly supports the disruption of the intramolecular hydrogen bond between boron-bound fluoride atoms and benzimidazole NH moiety upon interaction of BODIPY **1** with  $\text{F}^-$  ion, which is in agreement with the  $^1\text{H}$  NMR titration experiment.

We further tested BODIPY **1** for  $\text{F}^-$  sensing by following changes in the reduction potential of BODIPY **1** upon addition of increasing amounts of  $\text{F}^-$  by square wave voltammetry. The systematic changes in the reduction wave of BODIPY **1** upon increasing addition of  $\text{F}^-$  ion is shown in Figure 8. Progressive addition of  $\text{F}^-$  ion to BODIPY **1** resulted in a significant

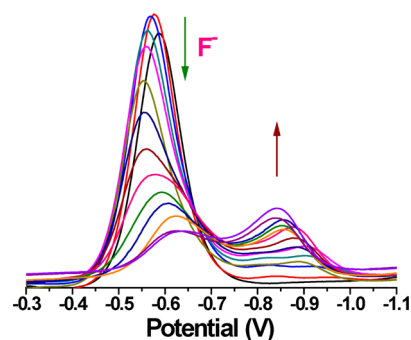
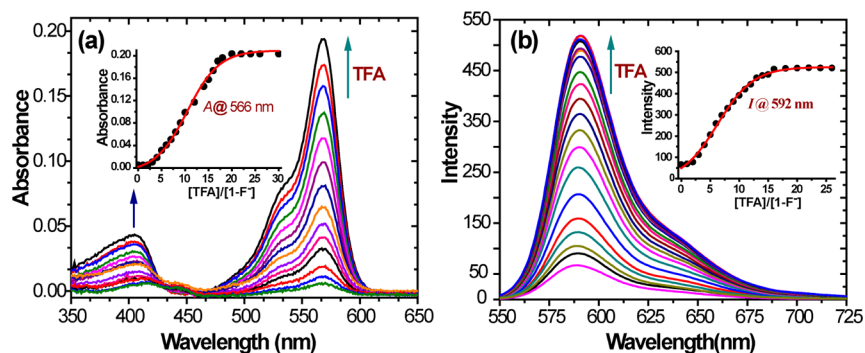


Figure 8. (a) Square wave voltammograms of BODIPY **1** (1.2 mM) in the presence of increasing amounts of  $\text{F}^-$  (TBAF) ions (0–1.2 equiv) in  $\text{CH}_3\text{CN}$  containing 0.1 M TBAP as supporting electrolyte recorded at  $50 \text{ mV s}^{-1}$  scan rate.

decrease of current intensity of reduction wave at  $-0.56$  V and at the same time appearance of new reduction with gradual increase in the current intensity at  $-0.85$  V. This significant shift of potential toward more negative by  $\sim 300$  mV indicates that  $\text{F}^-$  ion interaction enhances electron density on benzimidazole due to deprotonation. However, no change in the reduction of BODIPY **1** was observed upon addition of various other anions. These results supported the use of BODIPY **1** as a specific electrochemical sensor for  $\text{F}^-$  ion.

**Reversibility and Reusability of the Sensor.** It is very beneficial if a sensor can be reversible in nature and be reusable for sensing selective anion. A perusal of the literature revealed that most of the  $\text{F}^-$  ion sensors available in the literature are irreversible and can be used only one time. To test the reversibility and reusability of our BODIPY **1**, we carried out systematic titration studies of BODIPY **1-F}^-** complex upon addition of increasing amounts of TFA by absorption and fluorescence techniques. The absorption spectral titration of **1-F}^-** complex with increasing addition of TFA (0–12 equiv) in  $\text{CH}_3\text{CN}$  solution is shown in Figure 9a. Addition of increasing equivalents of TFA to a solution of **1-F}^-** complex resulted in the significant increase in the absorption bands at 566 and 428 nm. The sigmoidal nature of the plot of changes in the absorbance at 566 nm versus different equivalents of TFA shown as an inset in Figure 9a serves as an indicator of protonation of the imidazole moiety. Similarly, we also monitored the systematic titration studies of BODIPY **1-F}^-** complex upon addition of increasing equivalents of TFA by fluorescence studies in  $\text{CH}_3\text{CN}$  solution. Upon addition of increasing amounts of TFA to  $[\text{BODIPY } \mathbf{1-F}^-]$  complexes, the fluorescence emission gradually increased (Figure 9b), and 15-fold enhancement was observed on addition of 12 equiv of TFA. Thus, upon  $\text{F}^-$  ion addition, the benzimidazole moiety is electron-rich via deprotonation and engaged in photoinduced electron transfer (PET) quenching of the BODIPY excited state, and upon titration with TFA, the PET quenching is prevented because of protonation of benzimidazole group and the absorption and fluorescence properties were reverted (Scheme 2). We also studied the reversibility of the sensor upon addition of  $\text{F}^-$  ion and TFA in acetonitrile at different temperatures by employing fluorescence techniques. Initially, we have recorded the fluorescence spectra of BODIPY **1** upon addition  $\text{F}^-$  ion at various temperatures ranging from 25 to 60  $^\circ\text{C}$  (Figure S15a in SI) and our studies revealed that there is no significant effect of temperature on quenching of fluorescence of BODIPY **1**. Similarly, we also monitored the reversible



**Figure 9.** (a) Absorption and (b) emission spectral changes of BODIPY 1-F<sup>-</sup> solution (5 μM) upon addition of increasing equivalents of TFA (0–15 equiv) in CH<sub>3</sub>CN solution. The spectra were recorded after the addition of TFA to BODIPY 1 for 10 min. Excitation wavelength used was 530 nm.

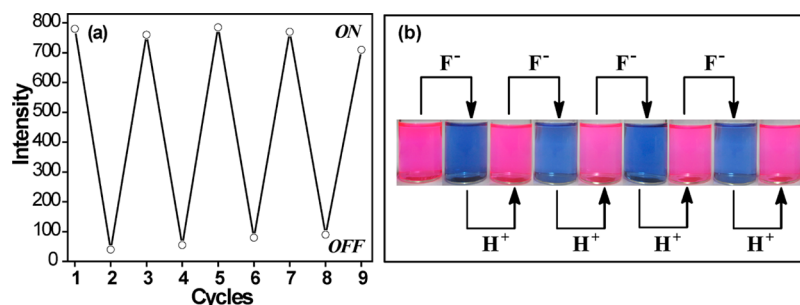


**Figure 10.** Fluorescence experiment showing the reversibility and reusability of the BODIPY 1 for sensing F<sup>-</sup> sequentially: (a) relative fluorescence intensity ( $\lambda_{\text{max}} = 592 \text{ nm}$ ) obtained during the titration of BODIPY 1 with F<sup>-</sup> and H<sup>+</sup> (TFA) in CH<sub>3</sub>CN solution; (b) visual color changes after each sequential addition of F<sup>-</sup> and H<sup>+</sup> ions.

phenomena by addition of TFA to a BODIPY 1-F<sup>-</sup> complex at different temperatures and studies clearly showed the recovery of fluorescence (Figure S15b in SI) occur indicating that BODIPY 1 can efficiently acts as a reversible probe even at variable temperatures.

The reversible and reusable response of BODIPY 1 was demonstrated by carrying out four alternate cycles of titration of BODIPY 1 with F<sup>-</sup> ion followed by addition of TFA (Figure 10). Titration of BODIPY 1 with F<sup>-</sup> ion resulted in quenching of fluorescence due to the formation of [BODIPY 1-F<sup>-</sup>] complex, thus acting as an OFF switch. However, titration of the [BODIPY 1-F<sup>-</sup>] complex with TFA resulted in protonation of the benzimidazole moiety and forms BODIPY 1, which is accompanied by significant increase in the fluorescence intensity, thus acting as an ON switch (Figure 10a). The repeated demonstration of the OFF/ON behavior of fluorescence as well as visual color changes from fluorescent pink to nonfluorescent blue and then back to fluorescence pink as shown in Figure 10b demonstrates the reversibility and reusability of sensor 1.

## CONCLUSIONS

In summary, we have synthesized benzimidazole substituted BODIPY 1 from 3,5-diformyl BODIPY 2 under simple reaction conditions. The presence of the benzimidazole moiety at the 3-position of BODIPY alters the electronic properties of the dye significantly. The absorption and emission bands were bathochromically shifted with decent quantum yield and longer singlet state lifetime compared to BODIPY 2. The crystal structure revealed that the BODIPY and benzimidazole moieties are in the same plane and showed the presence of intramolecular hydrogen bonding between benzimidazole NH

and boron-bound fluoride atoms. <sup>1</sup>H and <sup>19</sup>F NMR also supported the presence of intramolecular hydrogen bonding in BODIPY 1. We explored the potential use of benzimidazole substituted BODIPY for sensing anions by following various spectroscopic and electrochemical techniques. Our studies clearly showed that BODIPY 1 can act as a specific sensor for the detection of F<sup>-</sup> ion over various other anions. Addition of F<sup>-</sup> ions to a solution of BODIPY 1 led to a complete quenching of fluorescence of the BODIPY moiety accompanied by a visually detectable color change from fluorescent pink to nonfluorescent blue with a detection limit of 93 nM. Competitive binding experiments in the presence of various anions demonstrate that BODIPY 1 can specifically detect F<sup>-</sup> ions. Interestingly, systematic addition of TFA to non-fluorescent blue solution resulted in a change to fluorescent pink due to the significant enhancement of fluorescence intensity supporting the reversible nature of sensor 1. The reversibility and reusability of BODIPY 1 for sensing the F<sup>-</sup> ion has been demonstrated by sequential addition of F<sup>-</sup> ions followed by TFA over six cycles, which also indicates that BODIPY 1 can be used as a reversible and reusable sensor for F<sup>-</sup> ion.

## EXPERIMENTAL SECTION

The information regarding “Materials and Methods” and “X-ray Crystallography” was provided in the Supporting Information.

**General Procedure for Acetal Substituted BODIPY Imidazole (1).** A mixture of 3,5-diformyl BODIPY 2 (0.150 g, 1.03 mmol) and 1,2-phenylenediamine (0.05 g, 1.03 mmol) in dry methanol (15 mL) was warmed until some parts of the solids were dissolved, giving a bright yellow suspension. Neat TFA (0.1 g, 2.06 mmol) was added dropwise to yield a dark violet solution. The mixture was stirred for 1 h, and then a few drops of triethylamine were added to neutralize the

excess acid. The aldehydes present at 3 and 5 positions of BODIPY are highly reactive and electrophilic in nature. Since the reaction was carried out in methanol as solvent, the methanol acted as a nucleophile and reacted with one of the formyl groups and converted to acetal moiety. The crude product was purified using flash basic alumina column chromatography with petroleum ether/ethylacetate (90:10, v/v) and afforded pure BODIPY 1 as a golden yellow solid. Yield 38%. <sup>1</sup>H NMR (400 MHz, CDCl<sub>3</sub>, δ in ppm): 2.49 (s, 3H; -CH<sub>3</sub>), 3.51 (s, 6H; -OCH<sub>3</sub>), 6.01 (s, 1H; -CH), 6.76–6.78 (d, <sup>3</sup>J (H, H) = 4.32 Hz, 1H; py), 6.95–6.96 (d, <sup>3</sup>J (H, H) = 4.28 Hz, 1H; py), 7.04–7.05 (d, <sup>3</sup>J (H, H) = 4.52 Hz, 1H; py), 7.34–7.36 (d, <sup>3</sup>J (H, H) = 7.84 Hz, 4H; Ar), 7.47–7.49 (d, <sup>3</sup>J (H, H) = 8.04 Hz, 2H; Ar), 7.59–7.60 (d, <sup>3</sup>J (H, H) = 4.44 Hz, 1H; Py), 7.63–7.65 (d, <sup>3</sup>J (H, H) = 7.76 Hz, 1H; Ar), 7.84–7.86 (d, <sup>3</sup>J (H, H) = 7.92 Hz, 1H; Ar), 11.08 (br t, 1H; NH). <sup>11</sup>B NMR (128.3 MHz, CDCl<sub>3</sub>, δ in ppm): 0.31 (t, <sup>1</sup>J (B–F) = 33 MHz, 1B). <sup>19</sup>F NMR (376.4 MHz, CDCl<sub>3</sub>, δ in ppm): -137.7 (q, <sup>1</sup>J (F–B) = 33.4 MHz, 2F). <sup>13</sup>C NMR (100 MHz, CDCl<sub>3</sub>, δ in ppm): 14.3, 21.7, 22.9, 29.5, 29.9, 32.1, 54.0, 97.9, 118.4, 122.8, 125.1, 129.4, 130.8, 131.1, 131.9, 135.4, 141.6, 143.5. HRMS. Calcd for C<sub>26</sub>H<sub>24</sub>BF<sub>2</sub>N<sub>4</sub>O<sub>2</sub> [(M+1)<sup>+</sup>]: m/z 473.1960. Found: m/z 473.1953. Anal. Calcd for C<sub>26</sub>H<sub>23</sub>BF<sub>2</sub>N<sub>4</sub>O<sub>2</sub>: C, 66.12; H, 4.91; N, 11.86. Found: C, 66.27; H, 5.11; N, 11.73.

## ■ ASSOCIATED CONTENT

### Supporting Information

“Materials and Methods” and “X-ray Crystallography” and characterization data for the synthesized new compound, and spectroscopic data related to F-ion sensing. This material is available free of charge via the Internet at <http://pubs.acs.org>.

## ■ AUTHOR INFORMATION

### Corresponding Author

\*E-mail: [ravikanth@chem.iitb.ac.in](mailto:ravikanth@chem.iitb.ac.in).

### Notes

The authors declare no competing financial interest.

## ■ ACKNOWLEDGMENTS

M.R. thanks the Department of Atomic Energy (India) for financial support and S.M. acknowledge the IIT Bombay for PhD fellowships.

## ■ REFERENCES

- (1) (a) Waldbott, G. *Clin. Toxicol.* **1981**, *18*, 531–541. (b) Matuso, S.; Kiyomiya, K.-i.; Kurebe, M. *Arch. Toxicol.* **1998**, *72*, 798–806. (c) Zhang, S.-W.; Swager, T. M. *J. Am. Chem. Soc.* **2003**, *125*, 3420–3421.
- (2) (a) Riggs, B. L. *Bone Miner. Res.* **1984**, 366–393. (b) Laisalmi, M.; Kokki, H.; Soikkeli, A.; Markkanen, H.; Yli-Hankala, A.; Rosenberg, P.; Lindgren, L. *Acta Anaesthesiol. Scand.* **2006**, *50*, 982–987.
- (3) Zhang, C.; Suslick, K. S. *J. Am. Chem. Soc.* **2005**, *127*, 11548–11554.
- (4) (a) Amendola, V.; Gomez, D. E.; Fabbri, L.; Licchelli, M. *Acc. Chem. Res.* **2006**, *39*, 343–353. (b) Boiocchi, M.; Boca, L. D.; Gomez, D. E.; Fabbri, L.; Licchelli, M.; Monzani, E. *J. Am. Chem. Soc.* **2004**, *126*, 16507–16514. (c) Gomez, D. E.; Fabbri, L.; Licchelli, M. *J. Org. Chem.* **2005**, *70*, 5717–5720.
- (5) (a) Perez-Casas, C.; Yatsimirsky, A. K. *J. Org. Chem.* **2008**, *73*, 2275–2284. (b) Thiagarajan, V.; Ramamurthy, P.; Thirumalai, D.; Ramakrishnan, V. T. *Org. Lett.* **2005**, *7*, 657–660. (c) Wu, Y.; Peng, X.; Fan, J.; Gao, S.; Tian, M.; Zhao, J. *J. Org. Chem.* **2007**, *72*, 62–70. (d) Xu, G.; Tarr, M. A. *Chem. Commun.* **2004**, 1050–1051.
- (6) (a) Batista, R. M. F.; Oliveira, E.; Costa, S. P. G.; Lodeiro, C.; Raposo, M. M. M. *Org. Lett.* **2007**, *9*, 3201–3204. (b) Evans, L. S.; Gale, P. A.; Light, M. E.; Quesada, R. *Chem. Commun.* **2006**, 965–967. (c) Kim, S. K.; Bok, J. H.; Bartsch, R. A.; Lee, J. Y.; Kim, J. S. *Org. Lett.* **2005**, *7*, 4839–4842. (d) Liu, B.; Tian, H. *J. Mater. Chem.* **2005**, *15*,

2681–2686. (e) Peng, X.; Wu, Y.; Fan, J.; Tian, M.; Han, K. *J. Org. Chem.* **2005**, *70*, 10524–10531.

(7) (a) Lee, D. H.; Lee, H. Y.; Lee, K. H.; Hong, J.-I. *Chem. Commun.* **2001**, 1188–1189. (b) Lee, D. H.; Lee, K. H.; Hong, J.-I. *Org. Lett.* **2001**, *3*, 5–8. (c) Zhang, X.; Guo, L.; Wu, F.; Jiang, Y.-B. *Org. Lett.* **2003**, *5*, 2667–2670.

(8) (a) Hudnall, T. W.; Chiu, C.-W.; Gabbai, F. P. *Acc. Chem. Res.* **2009**, *42*, 388–397. (b) Hudnall, T. W.; Gabbai, F. P. *Chem. Commun.* **2008**, 4596–4597. (c) Lee, M. H.; Agou, T.; Kobayashi, J.; Kawashima, T.; Gabbai, F. P. *Chem. Commun.* **2007**, 1133–1135.

(9) (a) Miyaji, H.; Kim, H.-K.; Sim, E.-K.; Lee, C.-K.; Cho, W.-S.; Sessler, J. L.; Lee, C.-H. *J. Am. Chem. Soc.* **2005**, *127*, 12510–12512. (b) Sessler, J. L.; Kim, S. K.; Gross, D. E.; Lee, C.-H.; Kim, J. S.; Lynch, V. M. *J. Am. Chem. Soc.* **2008**, *130*, 13162–13166. (c) Gale, P. A. *Chem. Soc. Rev.* **2010**, *39*, 3746–377. (d) Gale, P. A. *Chem. Commun.* **2011**, 47, 82–86. (e) Gale, P. A. *Acc. Chem. Res.* **2006**, *39*, 465–475. (f) Sessler, J. L.; Gross, D. E.; Cho, W.-S.; Lynch, V. M.; Schmidtchen, F. P.; Bates, G. W.; Light, M. E.; Gale, P. A. *J. Am. Chem. Soc.* **2006**, *128*, 12281–12288.

(10) (a) Bozdemir, O. A.; Sozmen, F.; Buyukakir, O.; Guliyev, R.; Cakmak, Y.; Akkaya, E. U. *Org. Lett.* **2010**, *12*, 1400–1403. (b) Cao, X.; Lin, W.; Yu, Q.; Wang, J. *Org. Lett.* **2011**, *13*, 6098–6101. (c) Madhu, S.; Ravikanth, M. *Inorg. Chem.* **2012**, *51*, 4285–4292. (d) Rao, M. R.; Mobin, S. M.; Ravikanth, M. *Tetrahedron* **2010**, *66*, 1728–1734.

(11) (a) Lin, C.-L.; Selvi, S.; Fang, J.-M.; Chou, P.-T.; Lai, C.-H.; Cheng, Y.-M. *J. Org. Chem.* **2007**, *72*, 3537–3542. (b) Wang, J.; Yang, L.; Hou, C.; Cao, H. *Org. Biomol. Chem.* **2012**, *10*, 6271–6274. (c) Qu, Y.; Hua, J.; Tian, H. *Org. Lett.* **2010**, *12*, 3320–3323. (d) Schmidt, H. C.; Reuter, L. G.; Hamacek, J.; Wengner, O. S. *J. Org. Chem.* **2011**, *76*, 9081–9085.

(12) (a) Li, Y.; Cao, L.; Tian, H. *J. Org. Chem.* **2006**, *71*, 8279–8282. (b) Badr, I. H. A.; Meyerhoff, M. E. *J. Am. Chem. Soc.* **2005**, *127*, 5318–5319. (c) Aboubakr, H.; Brisset, H.; Siri, O.; Raimundo, J.-M. *Anal. Chem.* **2013**, *85*, 9968–9974.

(13) (a) Madhu, S.; Rao, M. R.; Shaikh, M. S.; Ravikanth, M. *Inorg. Chem.* **2011**, *50*, 4392–4400. (b) Lakshmi, V.; Ravikanth, M. *J. Org. Chem.* **2011**, *76*, 8466–8471. (c) Madhu, S.; Gonnade, R.; Ravikanth, M. *J. Org. Chem.* **2013**, *78*, 5056–5060. (d) Rao, M. R.; Tiwari, M. D.; Bellare, J. R.; Ravikanth, M. *J. Org. Chem.* **2011**, *76*, 7263–7268.

(14) (a) Loudet, A.; Burgess, K. *Chem. Rev.* **2007**, *107*, 4891–4932. (b) Ulrich, G.; Ziessel, R.; Harriman, A. *Angew. Chem., Int. Ed.* **2008**, *47*, 1184–1201. (c) Boens, N.; Leen, V.; Dehaen, W. *Chem. Soc. Rev.* **2012**, *41*, 1130–1172.

(15) (a) Olivier, J.-H.; Haefele, A.; Retailleau, P.; Ziessel, R. *Org. Lett.* **2010**, *12*, 408–411. (b) Nepomnyashchii, A. B.; Cho, S.; Rossky, P. J.; Bard, A. J. *J. Am. Chem. Soc.* **2010**, *132*, 17550–17559. (c) Murtagh, J.; Frimannsson, D. O.; O’Shea, D. F. *Org. Lett.* **2009**, *11*, 5386–5389. (d) Rihn, S.; Erdem, M.; Nicola, A. D.; Retailleau, P.; Ziessel, R. *Org. Lett.* **2011**, *13*, 916–919. (e) Palma, A.; Alvarez, L. A.; Scholz, D.; Frimannsson, D. O.; Grossi, M.; Quinn, S. J.; O’Shea, D. F. *J. Am. Chem. Soc.* **2011**, *133*, 19618–19621. (f) He, H.; Lo, P.-C.; Yeung, S.-L.; Fong, W.-P.; Ng, D. K. P. *Chem. Commun.* **2011**, 47, 4748–4750.

(16) (a) Ziessel, R.; Harriman, A. *Chem. Commun.* **2011**, 47, 611–631. (b) Harriman, A.; Mallon, L. J.; Goeb, S.; Ulrich, G.; Ziessel, R. *Chem.—Eur. J.* **2009**, *15*, 4553–4564. (c) Bura, T.; Retailleau, P.; Ziessel, R. *Angew. Chem., Int. Ed.* **2010**, *49*, 6659–6663. (d) Domaille, D. W.; Zeng, L.; Chang, C. J. *J. Am. Chem. Soc.* **2010**, *132*, 1194–1195. (e) Sun, Z.-N.; Wang, H.-L.; Liu, F.-Q.; Chen, Y.; Tam, P. K. H.; Yang, D. *Org. Lett.* **2009**, *11*, 1887–1890. (f) Leen, V.; Miscoria, D.; Yin, S.; Filarowski, A.; Ngongo, J. M.; Auweraer, M. V.; Boens, N.; Dehaen, W. *J. Org. Chem.* **2011**, *76*, 8168–8176. (g) Leen, V.; Braeken, E.; Luckermans, K.; Jackers, C.; Auweraer, M. V.; Boens, N.; Dehaen, W. *Chem. Commun.* **2009**, 4515–4517.

(17) (a) Jia, C.; Wu, B.; Liang, J.; Huang, X.; Yang, X.-J. *J. Fluoresc.* **2010**, *20*, 291–297. (b) Swamy, K. M. K.; Lee, Y. J.; Lee, H. N.; Chun, J.; Kim, Y.; Kim, S.-J. *J. Org. Chem.* **2006**, *71*, 8626–8628.